までに4つの疾患遺伝子を発見している[4~7]．

今回我々は，ノックアウトマウスの解析を起点としたヒトとマウスの融合遺伝学的アプローチにより，周産期に死亡する重篤な骨系統疾患である蝸牛様骨盤異形成症（OMIM：269250）の原因遺伝子 *SLC35D1*（solute carrier 35D1）を発見した[8]．これは，糖ヌクレオチドの輸送に関与する全く新しいタイプの骨系統疾患の原因遺伝子であった．

軟骨細胞外マトリックスと SLC35D1

軟骨には，細胞外マトリックスに糖タンパク質の一種であるプロテオグリカンが豊富に存在し，軟骨組織が受ける圧力を吸収するなど重要な役割を担っている[9]．プロテオグリカンは，タンパク質（コアタンパク質）にグルコサミノグリカンという糖鎖がたくさん結合した構造を持つ高分子ファミリー分子の総称である．グルコサミノグリカンは，アミノ糖（N-アセチルグルコサミンまたは N-アセチルガラクトサミン）とウロン酸（グルクロン酸またはイズロン酸）の2つの種類の糖の繰り返し構造からなり，軟骨細胞の小胞体やゴルジ体などの細胞内小器官内で活性化された糖ヌクレオチドをもとに合成される（図1）．その際，細胞質で作られた活性化糖ヌクレオチドを，膜を越えて細胞内小器官内へ運び込む必要がある．その役割を担っているのが糖ヌクレオチド輸送体の SLC35 で，ヒトでは 17 個の遺伝子が知られている[10]．SLC35D1 は，グルコサミノグリカンのうち主にコンドロイチン硫酸（CS）とヘパラン硫酸の合成に用いられる糖ヌクレオチドを輸送することが知られていた[10]．しかし，その生体内の機能は全く不明であった．

Slc35d1 遺伝子ノックアウトマウス

我々は，胚性幹細胞（ES 細胞）を用いた相同組み換え法によって，*Slc35d1* 遺伝子をノックアウトしたマウスを作製した[8]．このマウスは顔，四肢，背骨の形成の異常を示し（図2），出生直後に呼吸不全により死亡した．マウスの成長軟骨を組織学的に調べたところ，軟骨細胞の形態異常（増殖層細胞の円形化，細胞柱の消失など），細胞外マトリックスの著しい減少，およびプロテオグリカン凝集体の減少があった．この結果より，*Slc35d1* がマウスの骨格形成，軟骨マトリックスの代謝に不可欠な分子であることが分かった．

軟骨プロテオグリカン凝集体の主成分は，アグリカンである．アグリカンのコアタンパク質には，100 本以上の CS 鎖が結合している．酵母細胞を使った試験管内の実験で，SLC35D1 は CS 鎖の合成に用いられる糖ヌクレオチドを輸送することが知られていた[10]．そこで，*Slc35d1* ノックアウトマウスの軟骨組織中の CS 鎖を測定したところ，含量は約 1/4 に，糖鎖長は半分に低下しており，短い CS 鎖が付加された異常なアグリカンが形成されていた．この結果から，SLC35D1 によって輸送される糖ヌクレオチドは軟骨の CS 鎖の合成に用いられており，正常な含量と正常な糖鎖長の CS 鎖がマウスの骨格形成に必須であることが分かった．

蝸牛様骨盤異形成症（Schneckenbecken dysplasia）

では，ヒトではどうであろうか？ *Slc35d1* ノックアウトマウスの骨格異常のパターン，成長軟骨の病理組織像を詳細に検討したところ，ヒトの致死性の骨系統疾患である蝸牛様骨盤異形成症の病像と，非常によく似ていることが分かった（図3）．蝸牛様骨盤異形成症は，妊娠後期から新生児早期までの周産期に死亡する重篤な骨系統疾患で，常染色体劣性の遺伝形式をとる[11,12]．Schneckenbecken とは，ドイツ語で蝸牛（かたつむり）のような骨盤（Schneck＝蝸牛，Becken＝骨盤）と

図1 SLC35D1の機能とその異常（*Slc35d1*遺伝子ノックアウトマウス，蝸牛様骨盤異形成症）による疾患発症のメカニズム

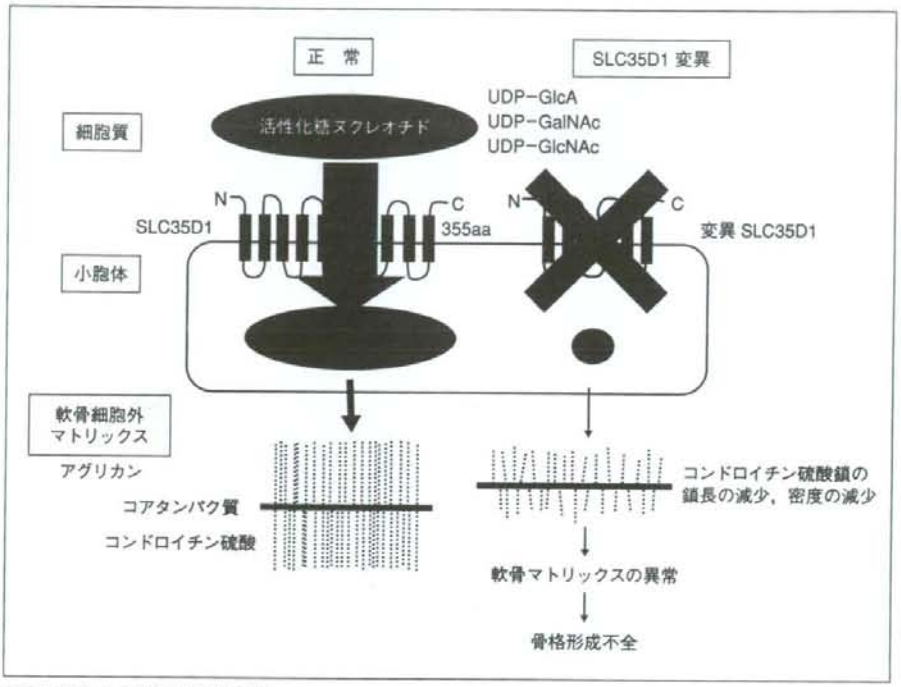

略語：巻末の「今月の略語」参照

いう意味で，骨盤を構成する腸骨という骨が特徴的な形をしていることに由来する[1]．

*SLC35D1*遺伝子変異の同定と変異タンパク質の機能解析

蝸牛様骨盤異形成症の患者ゲノムを用いて*SLC35D1*遺伝子の変異を調べた結果，2例でナンセンス変異を見つけた[8]．1例は血族結婚による founder 変異のホモ接合体で，1塩基の挿入によるフレームシフトによるナンセンス変異（c.125delA；p.S42fsX9）を持っていた．もう1例は複合ヘテロ接合体で，ナンセンス変異（c.932G>A；p.W311X）とエキソン-イントロン境界の点変異（IVS7+1 G>T）を持っていた．後者の変異はスプライス異常を起こし，ナンセンス変異を生じた（K212ins7X）．

いずれの変異も，C末端側を欠く短いSLC35D1タンパク質を生じ，*SLC35D1*の機能不全を起こすと予測された．そこで，酵母を使った実験系でこの変異タンパク質の糖ヌクレオチド輸送機能を調べると，輸送機能を完全に欠損していることが分かった．すなわちマウスと同様にヒトでも，SLC35D1の機能の欠損は重度の骨格の形成異常を引き起こすことが証明された（図1）．

さらに蝸牛様骨盤異形成症の患者ゲノムを収集し，*SLC35D1*遺伝子変異の解析を続けたところ，新たに3例で計3つの変異を同定した．ナンセンス変異（c.319C>T；p.

図2 *Slc35d1* 遺伝子ノックアウトマウスは重度の骨軟骨異形成症を示す

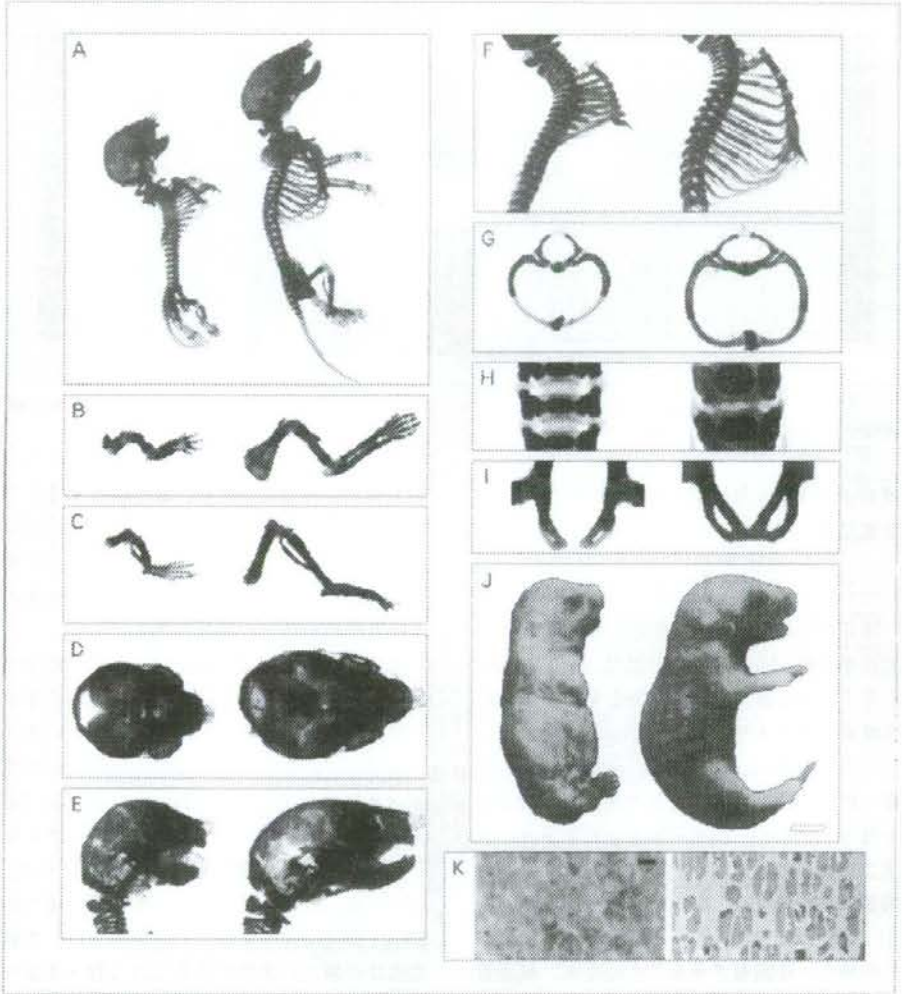

右：野生型，左：*Slc35d1* 遺伝子ノックアウトマウス．
A：骨格全身像，B：上肢，C：下肢，D：頭蓋前後像，E：頭蓋側面像，F：脊椎と肋骨，G：胸郭，H：腰椎正面像，I：骨盤，J：外観，K：成長軟骨（増殖層）の病理組織像．

R107X），種を越えてよく保存されたアミノ酸のミスセンス変異（c. 193A>C；p. T65P），およびフレームシフトと，それによるナンセンス変異を生じる1つのエキソンを含んだ4,959bp 欠失であった（IVS6＋730_IVS7＋3171del4959；p. R178fsX15）．*in vitro* の機能解析により，ミスセンス変異によって生じる SLC35D1 タンパク質も，糖ヌクレオチド輸送機能をほぼ完全に欠損した（古市ら，投稿中）．すなわち，これまでに発見された6

図3 蝸牛様骨盤異形成症（Schneckenbecken dysplasia）の表現型

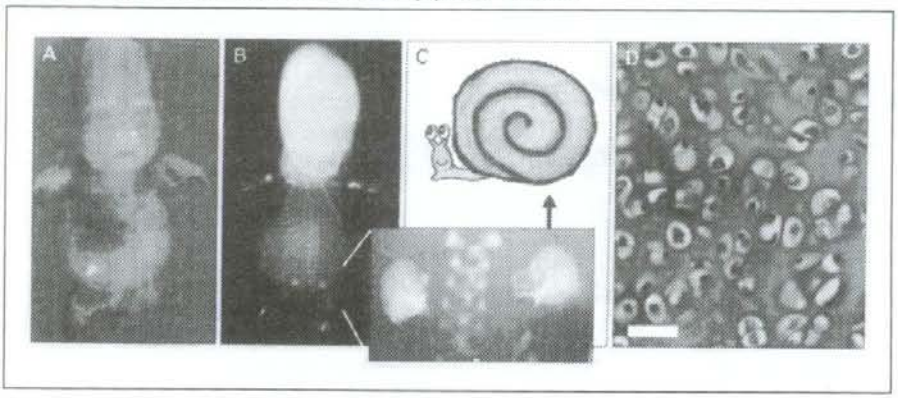

A：外見．B：X線像（全身正面像）．C：骨盤正面像．「蝸牛/かたつむりのような骨盤」．D：成長軟骨の増殖層の軟骨細胞．細胞は丸く細胞外マトリックスに乏しい．柱状配列が消失している．

種の *SLC35D1* 遺伝子変異はすべて機能喪失変異であった．

おわりに

多くの骨系統疾患で疾患遺伝子が見つかり，遺伝子診断が可能になって患者，家族に福音を与えているが，周産期に死亡する重症の骨系統疾患ではまだ疾患遺伝子が見つかっていないものが多い．このため，予後の推定，治療方針の決定，再発リスクの評価，遺伝カウンセリングなど，周産期医療や日常診療のさまざまな局面で問題が生じている．今回の原因遺伝子の発見は，蝸牛様骨盤異形成症の遺伝子診断，保因者診断を可能とし，この分野の医療を一歩前進させることになる．疾患遺伝子の同定によって蝸牛様骨盤異形成症の病態，発症のメカニズムの解明が進み，将来的には治療につながることが期待できる．また骨系統疾患では，分類上同じグループに属する表現型の類似した疾患では，多くの場合，類似した遺伝子に異常が見つかってきた．今後，蝸牛様骨盤異形成症の属する重症脊椎異形成症（severe spondylodysplastic dysplasias）のグループの疾患（表1）をはじめとする蝸牛様骨盤異形成症の類縁疾患，ならびに SLC35D1 以外の糖ヌクレオチド輸送体，または CS 鎖の合成にかかわる遺伝子の変異を調べることによって，新たな骨系統疾患の原因遺伝子の発見が期待できる．

今回の研究成果は，SLC35D1 などのヌクレオチド輸送体や CS 鎖合成に携わる分子が軟骨代謝，骨格形成に密接に関与していることを示している．近年，変形性関節症や椎間板ヘルニアなどの骨・関節の common disease と，グルコサミンやコンドロイチンなど糖鎖との関係が巷間の注目を浴びている．骨格形成，軟骨代謝における糖鎖の機能への糖鎖生物学的観点からのアプローチは，高齢化社会の最大の課題であるこれら骨・関節疾患の病態の解明に不可欠で，その画期的な治療薬・治療法の開発につながる可能性を持っている．*Slc35d1* 遺伝子ノックアウトマウスは，これらの研究のための良いモデルとなる可能性を持っている．

謝　辞

本研究は，以下に挙げた国内外の多くの研究者との共同研究による（敬称略），理化学研究所免

疫アレルギー研究センター 免疫器官形成研究グループ（古関明彦，平岡秀一），東京医科歯科大学医歯学総合研究科分野（柴田俊一，柳下正樹），千葉大学薬学部分子創薬科学研究部門（豊田英尚，豊田亜希子），東京都臨床医学総合研究所生命情報研究部門（佐内 豊，石田信宏），Cedars-Sinai Medical Center, UCLA (David L. Rimoin, Daniel H. Cohn), Department of Pathology, University Medical Center Utrecht (Peter G. Nikkels), Centre for Pediatrics and Adolescent Medicine, Freiburg University Hospital (Andrea Superti-Furga, Sheila Unger).

文　献

1) 西村 玄: 骨系統疾患X線アトラス. 医学書院, 東京, 1993.
2) 池川志郎: 軟骨関連遺伝子異常と骨系統疾患. 現代医療 33 (5): 1171-1178, 2001.
3) Superti-Furga A, et al: Nosology and classification of genetic skeletal disorders: 2006 revision. Am J Med Genet A 143 (1): 1-18, 2007.
4) Ikegawa S, et al: Mutation of the type X collagen gene (COL10A1) causes spondylometaphyseal dysplasia. Am J Hum Genet 63 (6): 1659-1662, 1998.
5) Kinoshita A, et al: Domain-specific mutations in TGFB1 result in Camurati-Engelmann disease. Nat Genet 26 (1): 19-20, 2000.
6) Nishimura G, et al: Identification of COL2A1 mutations in platyspondylic skeletal dysplasia, Torrance type. J Med Genet 41 (1): 75-79, 2004.
7) Nishimura G, et al: The Shwachman-Bodian-Diamond syndrome gene mutations cause a neonatal form of spondylometaphysial dysplasia (SMD) resembling SMD Sedaghatian type. J Med Genet 44 (4): e73, 2007.
8) Hiraoka S, et al: Nucleotide-sugar transporter SLC35D1 is critical to chondroitin sulfate synthesis in cartilage and skeletal development in mouse and human. Nat Med 13 (11): 1363-1367, 2007.
9) Knudson C B, et al: Cartilage proteoglycans. Semin Cell Dev Biol 12 (2): 69-78, 2001.
10) Ishida N, et al: Molecular physiology and pathology of the nucleotide sugar transporter family (SLC35). Pflugers Arch 447 (5): 768-775, 2004.

SLC35D1 that Encodes a Nucleotide Sugar Transporter is the Disease Gene for Schneckenbecken Dysplasia

Shiro Ikegawa[1,2], Tatsuya Furuichi[1], Gen Nishimura[2,3]
[1] Laboratory for Bone and Joint Diseases, Center for Genomic Medicine, RIKEN
[2] Japanese Consortium for Skeletal Dysplasia
[3] Department of Radiology, Tokyo Metropolitan Kiyose Children's Hospital

J Hum Genet (2008) 53:764–768
DOI 10.1007/s10038-008-0305-z

A compound heterozygote of novel and recurrent *DTDST* mutations results in a novel intermediate phenotype of Desbuquois dysplasia, diastrophic dysplasia, and recessive form of multiple epiphyseal dysplasia

Atsushi Miyake · Gen Nishimura · Toru Futami · Hirofumi Ohashi · Kazuhiro Chiba · Yoshiaki Toyama · Tatsuya Furuichi · Shiro Ikegawa

Received: 27 March 2008 / Accepted: 19 May 2008 / Published online: 14 June 2008

Abstract Diastrophic dysplasia sulfate transporter (DTDST) is required for synthesis of sulfated proteoglycans in cartilage, and its loss-of-function mutations result in recessively inherited chondrodysplasias. The 40 or so *DTDST* mutations reported to date cause a group of disorders termed the diastrophic dysplasia (DTD) group. The group ranges from the mildest recessive form of multiple epiphyseal dysplasia (r-MED) through the most common DTD to perinatally lethal atelosteogenesis type II and achondrogenesis 1B. Furthermore, the relationship between *DTDST* mutations, their sulfate transport function, and disease phenotypes has been described. Here we report a girl with *DTDST* mutations: a compound heterozygote of a novel p.T266I mutation and a recurrent p.ΔV340 mutation commonly found in severe phenotypes of the DTD group. In infancy, the girl presented with skeletal manifestations reminiscent of Desbuquois dysplasia, another recessively inherited chondrodysplasia, the mutations of which have never been identified. Her phenotype evolved with age into an intermediate phenotype between r-MED and DTD. Considering her clinical phenotypes and known phenotypes of p.ΔV340, p.T266I was predicted to be responsible for mild phenotypes of the DTD group. Our results further extend the phenotypic spectrum of DTDST mutations, adding Desbuquois dysplasia to the list of differential diagnosis of the DTD group.

Keywords Diastrophic dysplasia sulfate transporter (DTDST) · Diastrophic dysplasia (DTD) · Recessive form of multiple epiphyseal dysplasia (r-MED) · Desbuquois dysplasia · Genotype–phenotype correlation

A. Miyake · T. Furuichi · S. Ikegawa (✉)
Laboratory for Bone and Joint Diseases,
Center for Genomic Medicine, RIKEN, 4-6-1 Shirokanedai,
Minato-ku, Tokyo 108-8639, Japan
e-mail: sikegawa@ims.u-tokyo.ac.jp

G. Nishimura
Department of Radiology, Tokyo Metropolitan Kiyose
Children's Hospital, Kiyose, Tokyo, Japan

T. Futami
Department of Orthopaedic Surgery,
Shiga Medical Center for Children,
Moriyama, Shiga, Japan

H. Ohashi
Department of Heredity Clinic,
Saitama Children's Medical Center,
Saitama, Japan

A. Miyake · K. Chiba · Y. Toyama
Department of Orthopaedic Surgery,
Keio University School
of Medicine, Shinjuku, Tokyo, Japan

Introduction

The diastrophic dysplasia sulfate transporter gene (*DTDST*, alias *SLC26A2*) encodes membrane protein with 12 transmembrane domains composed of 739 amino acids. DTDST transports sulfate and contributes to synthesis of sulfated proteoglycans in cartilage. Approximately 40 *DTDST* mutations have been reported (Rossi and Superti-Furga 2001) in four autosomal recessive chondrodysplasias, including two nonlethal disorders, a recessive form of multiple epiphyseal dysplasia (r-MED) (Superti-Furga et al. 1999), and diastrophic dysplasia (DTD) (Hastbacka et al. 1994); and two lethal disorders, atelosteogenesis type II (AO-II) (Hastbacka et al. 1996) and achondrogenesis 1B (ACG-1B) (Superti-Furga et al. 1996a). These disorders constitute a disease spectrum termed the diastrophic

dysplasia (DTD) group (Lachman 1998; Hall 2002; Superti-Furga et al. 2007).

DTDST mutations result in reduction in either sulfate uptake or proteoglycan sulfation. In fact, chondrocytes and cartilage matrices with chondrodysplasias with *DTDST* mutations show a deficiency of intracellular sulfate and extracellular proteoglycan (Hastbacka et al. 1996; Superti-furga et al. 1996a; Rossi et al. 1997, 1998). Investigation for sulfate transporter function and cell localization of mutant DTDSTs have revealed that *DTDST* mutations are classifiable into partial-function mutations and null mutations (Karniski 2001, 2004; Maeda et al. 2006). Partial-function mutants have 39–69% sulfate transport activity compared with the wild-type DTDST (Karniski 2004). These mutant proteins are properly expressed on the cell membrane, but they are significantly less than the wild-type protein. Null mutations including p.ΔV340 create trace amounts of proteins either from poor expression or from rapid degradation. These proteins are expressed only intracellularly, not on the plasma membrane (Karniski 2004).

The genotype–phenotype correlation of *DTDST* mutations has been well described (Superti-Furga et al. 1996b; Rossi and Superti-Furga 2001; Karniski 2001, 2004). The current concept includes homozygotes for null mutations resulting in ACG-1B, heterozygotes for both null and partial-function mutations in either AO-II or DTD, and homozygotes for partial-function mutations in r-MED. However, some variants of these diseases, such as McAlister dysplasia as a variant of AO-II (Rossi et al. 1997) and broad bone platyspondyly as a variant of DTD (Mégarbané et al. 1999), have also been described. Thus, the spectrum of phenotypes caused by *DTDST* mutations may extend further.

Desbuquois dysplasia is a rare, nonlethal, autosomal recessive disease, and its causative gene was hitherto unknown. Desbuquois dysplasia is characterized by marked short stature of prenatal onset, joint laxity, round face, bulging eyes, midface hypoplasia, "Swedish-key" appearance of the proximal femora, hyperphalangy of the index finger, and advanced carpal and tarsal bone ossification (Faivre et al. 2004). The phenotypic variations are diverse, and mild Desbuquois dysplasia without hyperphalangy has been reported (Nishimura et al. 1999). The phenotype variations cause diagnostic confusion, and Desbuquois dysplasia is occasionally misdiagnosed as other chondrodysplasias such as Larsen syndrome.

Here we report an unusual phenotype in a compound heterozygote of a novel p.T266I mutation and a common p.ΔV340 mutation. The phenotype was indistinguishable in infancy from that of Desbuquois dysplasia, but it evolved into an intermediate between r-MED and DTD. Our experience raises the possibility of a novel phenotype generated by a novel *DTDST* mutation and implies difficulty in differential diagnosis between Desbuquois dysplasia and mild phenotypes in the DTD group on clinical and radiological grounds.

Materials and methods

Clinical report

The girl was born to a healthy nonconsanguineous Japanese couple by normal delivery at 40 weeks gestation. Her birth height was 49.5 cm. She had bilateral clubfeet, contracture of the MP joints, and hyperextension of bilateral knees. She also had short limbs involving all segments. The midface was somewhat flattened. Radiographs at 2 weeks of age revealed mildly broadened long bones of the legs, bilateral hip subluxation, and bilateral reduction in the talocalcaneal angles of the feet. Radiographs at 7 months of age showed broadening and Swedish-key appearance of the proximal femora and advanced carpal bone ossification (Fig. 1), which led to a diagnosis of Desbuquois dysplasia. Short stature became obvious at 3 years of age and was remarkable at 4 years of age (88 cm: −3 SD). On radiological examination at 4 years of age, our attention was drawn to proximal femoral epiphyseal dysplasia and broadening of the short tubular bones, resembling those of r-MED (Fig. 2). The findings led us to a molecular analysis of the *DTDST*.

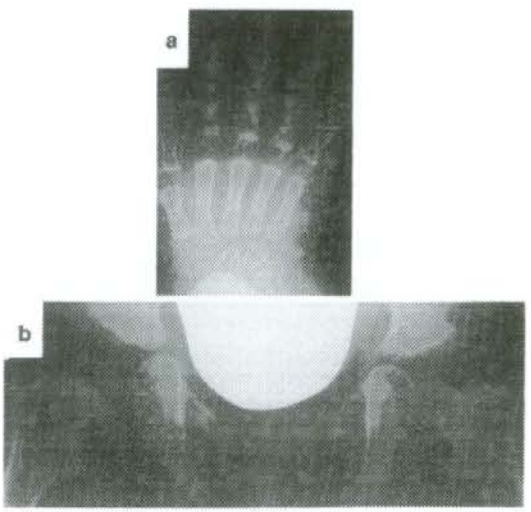

Fig. 1 X-rays at 7 months of age. **a** Metacarpal bones and phalanges were broad. Four carpal bones were visible, indicating that carpal bone ossification was advanced. **b** Swedish-key appearance of proximal femora were visible

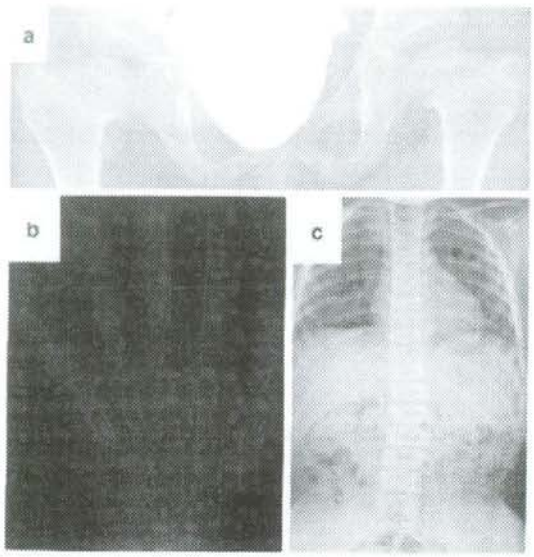

Fig. 2 X-rays at 4 years of age. **a** Bilateral hip joints had acetabular dysplasia. Femoral heads were slightly flat and femoral necks were broad. As a result, coxa vara was displayed. **b** Carpal bone ossification was advanced; seven carpal bones were visible in this 4-year-old hand. **c** Total spine showed mild scoliosis and mild flattening of vertebrae

Detection of mutations

Peripheral blood samples of the patient, her parents, and 96 unrelated normal Japanese controls were obtained with written informed consent. Genomic deoxyribonucleic acid (DNA) samples were extracted by standard procedures. The entire coding region and flanking intronic regions were examined by polymerase chain reaction (PCR) and direct sequence analysis (Ikeda et al. 2001). Direct sequencing was performed using an ABI prism 3700 automated sequencer (Applied Biosystems, Foster City, CA, USA). To obtain allelic information, PCR products containing mutations were cloned using a TOPO TA cloning kit (Invitrogen, Carlsbad, CA, USA) and sequenced. The paternity was confirmed by ten unlinked microsatellite markers. They were genotyped using an ABI prism linkage mapping set v2.5 and an ABI prism 3700 automated sequencer (Applied Biosystems) by standard procedures.

Evaluation of mutations

To investigate the conservation of mutated amino acids p.T266 and p.V340, reference sequences of human (NP_000103), horse (NP_001075403), mouse (NP_031911), chicken (XP_425183), and zebra fish (XP_685114) were obtained from the National Center for Biotechnology Information (http://www.ncbi.nlm.nih.gov/). PSORT, a computer program for the prediction of protein localization sites in cells (http://psort.nibb.ac.jp/), was used to predict the structure before and after introduction of p.T266I.

Table 1 A summary of mutations in this case

Nucleotide	Amino acid	dbSNP No	AF	Mutation DB
c.797C > T	p.T266I	(–)	(–)	(–)
c.1018–1020del	p.ΔV340	(–)	(–)	ACG1B, DTD
c.2065A > T	p.T689S	rs3776070	0.167	Polymorphism

p.ΔV340: a common mutation reported as null mutation (Karniski 2004)

ACG1B achondrogenesis 1B, *DTD* diastrophic dysplasia, *AF* allele frequency, (–) no data in database

Results

Detection of mutations

The entire coding region and flanking intronic regions of *DTDST* were directly sequenced. Two heterozygous mutations, c.797C > T (p.T266I) and c.1018-1020del (p.ΔV340), were detected (Table 1). The former was not found in the public database for single nucleotide polymorphism (SNP) and mutation or in 96 unrelated Japanese controls, whereas the latter was recurrent (Superti-Furga et al. 1996b). Polymerase chain reaction (PCR) products containing two mutations were cloned to obtain allelic information, and the patient was recognized as a compound heterozygote of the two mutations (Fig. 3a). The two mutations were searched in the parents by direct sequence. A heterozygous mutation of c.1018-1020del (p.ΔV340) was recognized in the mother, but neither of the mutations was found in the father (Fig. 3b). Paternity was confirmed by genotyping unlinked ten microsatellite markers for the patient and parents.

Evaluation of mutations

Amino acid sequences of DTDST were compared between five diverse species; p.T266 and p.V340 were conserved in all five species (Fig. 4a). Using PSORT, the structural change of DTDST protein was predicted. T266 was outside of the cell, but I266 was in the plasma membrane. The introduction of p.T266I caused ten-amino-acids shortening of the third cytoplasmic domain and ten-amino-acids elongation of the third extracellular domain of the DTDST protein (Fig. 4b).

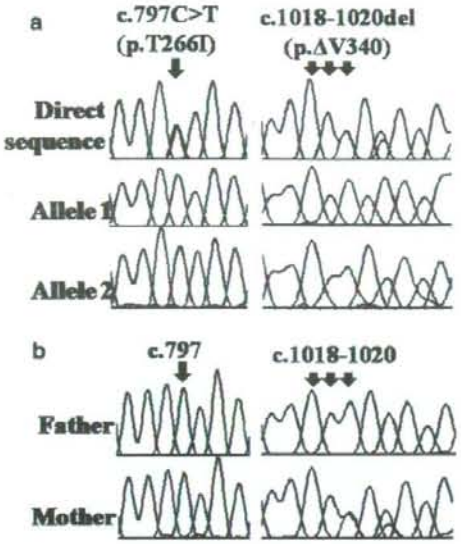

Fig. 3 **a** Sequences of the patient. *Top* direct sequence; *middle and bottom* sequences after TA cloning. The *red*, *blue*, *green*, and *black waves* represent nucleotides, thymine, cytosine, and adenine and guanine, respectively. The patient had heterozygous *DTDST* mutations, c.797C > T (p.T266I) and c.1018-1020del (p.ΔV340). **b** Direct sequences of the parents. The mother was a heterozygote of c.1018-1020del (p.ΔV340), but the father had neither of these two mutations

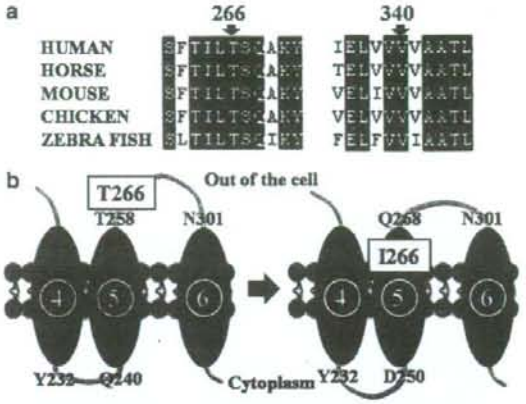

Fig. 4 Characterization of mutated amino acids. **a** Conservation of p.T266 and p.V340 in the diastrophic dysplasia sulfate transporter (DTDST) protein among different species. **b** Structural change of a DTDST protein predicted by PSORT. *Ellipses* represent the transmembrane domains, and *curved lines* represent either extracellular or cytoplasmic domains. The *plain numbers* are neighboring amino acid numbers of transmembrane domains shown at those positions. The *circled numbers* are transmembrane domain numbers from the N-terminus. If a 266th amino acid (*squared*) changed from threonine (*T*) to isoleucine (*I*), it would migrate from outside of the cell into the plasma membrane. The length of the fifth transmembrane domain would not change, but that of the neighboring third extracellular and third cytoplasmic domain would be shortened and elongated by ten amino acids, respectively

Discussion

r-MED and DTD are milder diseases in the DTD group. r-MED patients are not short, and they are healthy in childhood other than occasional associations with clubfeet and cleft palate. The radiological hallmarks include, as in the child in this study, broad proximal femora with proximal femoral epiphyseal dysplasia and undertubulated short tubular bones. By contrast, DTD presents with pre- and postnatal short stature, distinctive hitchhiker thumbs, inflammatory ear swelling, and intractable clubfeet, as well as joint dislocations and spinal malalignment. The skeletal changes are variable among affected individuals. Broad proximal femora and undertubulated short tubular bones are occasional, but not exclusive, findings. The presence of short stature and the radiological constellation of the child reported here fit an intermediate between r-MED and DTD.

Of note is that in this case, skeletal changes in infancy were reminiscent of Desbuquois dysplasia. r-MED and DTD also show broad proximal femora with prominence of the lesser trochanters, but those are not so prominent that are comparable to Swedish-key appearance. Mildly advanced carpal and tarsal ossifications are known in DTD but are not so prominent as those in this case or Desbuquois dysplasia.

c.1018-1020del (p.ΔV340) is a relatively common mutation in DTD and ACG-1B. Immunofluorescence analysis showed that p.ΔV340 was not on the plasma membrane, although DTDST was a plasma membrane protein. Therefore, it was classified as a null mutation and associated with severe phenotypes of the DTD group (Karniski 2004). c.797C > T (p.T266I) is a novel mutation, which is supported by its de novo occurrence during paternal gametogenesis. Conservation between diverse species suggests that p.T266 plays an important role in DTDST protein. T266 was predicted to be outside of the plasma membrane because of its OH base, which had no affinity to lipid but to H_2O. On the other hand, I266 was predicted to migrate in the plasma membrane because it had nonpolarity and high affinity to lipid. As a consequence, the structure of DTDST protein would change drastically, most likely affecting its sulfate transport function.

According to a previous report (Karniski 2004), nonlethal disorders caused by *DTDST* mutations would be either a heterozygote of partial-function mutation and null mutation or a homozygote of partial-function mutations. The phenotypes of the child in this study fell into the milder range of the DTD group, and she had p.ΔV340, a null mutation. Therefore, it seems that c.797C > T (p.T266I) is classifiable as partial-function mutation, the sulfate transport activity of which is only mildly affected

and in which localization is predicted to be on the plasma membrane. The result of the PSORT analysis supports this presumption. Further functional evidence is needed to validate the mutation function.

Thus, we first report a novel *DTDST* mutation, p.T266I, that results in a novel phenotype in combination with a recurrent null mutation, further extending the phenotypic spectrum of *DTDST* mutations. We hope that these findings will support clinical and genetic diagnosis of similar chondrodysplasias.

Acknowledgments We thank the patient and her parents for cooperation in the study. This work was supported by grant-in-aid from Development of New Approach for Regenerative Medicine.

References

Faivre L, Cormier-Daire V, Younf I, Bracq H, Finidori G, Padovani JP, Odent S, Lachman R, Munnich A, Maroteaux P, Le Merrer M (2004) Long-term outcome in Desbuquois dysplasia: a follow-up in four adult patients. Am J Med Genet A 124:54–59

Hall CM (2002) International nosology and classification of constitutional disorders of bone (2001). Am J Med Genet 113:65–77

Hastbacka J, de la Chapelle A, Mahtani MM, Clines G, Reeve-Daly MP, Daly M, Hamilton BA, Kusumi K, Trivedi B, Weaver A, Coloma A, Lovett M, Buckler A, Kaitila I, Lander ES (1994) The diastrophic dysplasia gene encodes a novel sulfate transporter: positional cloning by fine-structure linkage disequilibrium mapping. Cell 78:1073–1087

Hastbacka J, Superti-Furga A, Wilcox WR, Rimoin DL, Cohn DH, Lander ES (1996) Atelosteogenesis type II is caused by mutations in the diastrophic dysplasia sulfate-transporter gene (DTDST): evidence for a phenotypic series involving three chondrodysplasias. Am J Hum Genet 58:255–262

Ikeda T, Mabuchi A, Fukuda A, Hiraoka H, Kawakami A, Yamamoto S, Machida H, Takatori Y, Kawaguchi H, Nakamura K, Ikegawa S (2001) Identification of sequence polymorphisms in two sulfation-related genes, PAPSS2 and SLC26A2, and an association analysis with knee osteoarthritis. J Hum Genet 46:538–543

Karniski LP (2001) Mutations in the diastrophic dysplasia sulfate transporter (DTDST) gene: correlation between sulfate transport activity and chondrodysplasia phenotype. Hum Mol Genet 10:1485–1490

Karniski LP (2004) Functional expression and cellular distribution of diastrophic dysplasia sulfate transporter (DTDST) gene mutations in HEK cells. Hum Mol Genet 13:2165–2171

Lachman RS (1998) International nomenclature and classification of the osteochondrodysplasias (1997). Pediatr Radiol 28:737–744

Maeda K, Miyamoto Y, Sawaki H, Karniski LP, Nakashima E, Nishimura G, Ikegawa S (2006) A compound heterozygote harboring novel and recurrent *DTDST* mutations with intermediate phenotype between Atelosteogenesis type II and Diastrophic dysplasia. Am J Med Genet A 140:1143–1147

Mégarbané A, Haddad FA, Haddad-Zebouni S, Achram M, Eich G, Le Merrer M, Superti-Furga A (1999) Homozygosity for a novel DTDST mutation in a child with a 'broad bone-platyspondylic' variant of diastrophic dysplasia. Clin Genet 56:71–76

Nishimura G, Hong HS, Kawame H, Sato S, Cai G, Ozono K (1999) A mild variant of Desbuquois dysplasia. Eur J Pediatr 158:479–483

Rossi A, Superti-Furga A (2001) Mutations in the diastrophic dysplasia sulfate transporter (DTDST) gene (SLC26A2): 22 novel mutations, mutation review, associated skeletal phenotypes, and diagnostic relevance. Hum Mutat 17:159–171

Rossi A, Bonaventure J, Delezoide AL, Superti-Furga A, Cetta G (1997) Undersulfation of cartilage proteoglycans ex vivo and increased contribution of amino acid sulfur to sulfation in vitro in McAlister dysplasia/atelosteogenesis type 2. Eur J Biochem 248:741–747

Rossi A, Kaitila I, Wilcox WR, Rimoin DL, Steinmann B, Cetta G, Superti-Furga A (1998) Proteoglycan sulfation in cartilage and cell cultures from patients with sulfate transporter chondrodysplasias: relationship to clinical severity and indication on the role of intracellular sulfate production. Matrix Biol 17:361–369

Superti-Furga A, Hastbacka J, Wilcox WR, Cohn DH, van der Harten HJ, Rossi A, Blau N, Rimoin DL, Steinmann B, Lander ES, Gitzelmann R (1996a) Achondrogenesis type IB is caused by mutations in the diastrophic dysplasia sulphate transporter gene. Nat Genet 12:100–102

Superti-Furga A, Rossi A, Steinmann B, Gitzelmann R (1996b) A chondrodysplasia family produced by mutations in the diastrophic dysplasia sulfate transporter gene: genotype/phenotype correlations. Am J Med Genet 63:144–147

Superti-Furga A, Neumann L, Riebel T, Eich G, Steinmann B, Spranger J, Kunze J (1999) Recessively inherited multiple epiphyseal dysplasia with normal stature, club foot, and double layered patella caused by a DTDST mutation. J Med Genet 36:621–624

Superti-Furga A, Unger S, the Nosology group of the international skeletal dysplasia society (2007) Nosology and classification of genetic skeletal disorders: 2006 revision. Am J Med Genet A 143:1–18

American Journal of Medical Genetics Part A 146A:1458–1461 (2008)

Clinical Report

Cryptic 17q22 Deletion in a Boy With a t(10;17)(p15.3;q22) Translocation, Multiple Synostosis Syndrome 1, and Hypogonadotropic Hypogonadism

Reiko Shimizu,[1]* Norimasa Mitsui,[2] Yasuhiro Mori,[3] Shogen Cho,[3] Shunji Yamamori,[4] Makiko Osawa,[1] and Hirofumi Ohashi[2]

[1]Department of Pediatrics, School of Medicine, Tokyo Women's Medical University, Tokyo, Japan
[2]Division of Medical Genetics, Saitama Children's Medical Center, Saitama, Japan
[3]Department of Orthopedic Surgery, Teikyo University School of Medicine, Tokyo, Japan
[4]Molecular Genetic Testing Department, Mitsubishi Chemical Medience Corporation, Tokyo, Japan

Received 30 May 2007; Accepted 20 February 2008

We report on a boy who had multiple synostosis syndrome 1, an autosomal dominant disorder characterized by progressive symphalangism, multiple joint fusions, conductive deafness, and mild facial dysmorphism. In addition the boy developed delay of puberty, bone age, and closure of the epiphyseal lines of long bones with tall stature. These findings and decreased plasma LH and FSH levels at age 19 years were compatible with hypogonadotropic hypogonadism. G-banded chromosomes showed a balanced translocation t(10;17)(p15.3;q22). Chromosomal FISH analysis, using a series of BAC clones surrounding the translocation breakpoints, detected a 2.2–3.9 Mb deletion at 17q22. The deletion encompassed *NOG*, a gene responsible for multiple synostosis syndrome 1. It was assumed that a gene for pituitary secretion of gonoadotropic hormones was deleted at the 17q22 segment. © 2008 Wiley-Liss, Inc.

Key words: reciprocal translocation; cryptic deletion; hypogonadotropic hypogonadism; multiple synostosis syndrome 1; *NOG*

How to cite this article: Shimizu R, Mitsui N, Mori Y, Cho S, Yamamori S, Osawa M, Ohashi H. 2008. Cryptic 17q22 deletion in a boy with a t(10;17)(p15.3;q22) translocation, multiple synostosis syndrome 1, and hypogonadotropic hypogonadism. Am J Med Genet Part A 146A:1458–1461.

INTRODUCTION

Apparently "balanced" de novo translocations, when associated with abnormal phenotype, are frequently "unbalanced" with cryptic deletions, especially around the translocation breakpoints [Gribble et al., 2005; De Gregori et al., 2007]. Haploinsufficiency of dosage-sensitive genes in a deleted interval might cause a phenotype. Such disease-associated structural chromosomal rearrangements play an important role in positional cloning of many disease genes [Bugge et al., 2000]. Isolated hypogonadotropic hypogonadism is caused by mutations of at least four genes: the gonadotropin-releasing hormone receptor gene at 4q21 [de Roux et al., 1997], the fibroblast growth factor receptor-1 gene at 8p11 [Pitteloud et al., 2006], the nasal embryonic LHRH factor gene at 9q34 [Miura et al., 2004], and the G protein-coupled receptor-54 gene on 19p [Seminara et al., 2003].

We describe acryptic 17q22 deletion accompanying a de novo balanced reciprocal translocation in a boy with multiple synostosis syndrome 1 resulting from deletion of *NOG* at 17q22. The boy also developed hypogonadotropic hypogonadism. We will discuss the possibility of the presence of a gene for hypogonadotropic hypogonadism at 17q22.

CLINICAL REPORT

The patient, a Japanese boy, was delivered at term after an uncomplicated pregnancy with a weight of

Grant sponsor: Ministry of Health, Labour and Welfare of Japan; Grant number: H18-005; Grant sponsor: Kawano Masanori Memorial Foundation for Promotion of Pediatrics, Japan.

*Correspondence to: Reiko Shimizu, Department of Pediatrics, School of Medicine, Tokyo Women's Medical University, 8-1 Kawada-cho, Shinjuku-ku, Tokyo 160-0022, Japan. E-mail: rmuto@ped.twmu.ac.jp

Published online 30 April 2008 in Wiley InterScience (www.interscience.wiley.com)
DOI 10.1002/ajmg.a.32319

2,800 g. His parents and an older brother were healthy, of normal stature, and denied anosmia. In the neonatal period, inability to flex his fingers and limited movements of the hips, elbows, and jaw were noted. Partial conductive hearing loss, astigmatism, hyperopia and moderate developmental delay became increasingly obvious with advancing age. Stapedectomy at age 13 years resulted in improved language skill.

When first seen by us at age 13 years, he measured 171 cm (+1.5 SD). The proximal interphalangeal joints of his second to fifth fingers were fixed in extension, and skin creases over these joints were absent. The metacarpophalangeal joints of the third to fifth toes were fixed in extension and their proximal interphalangeal were fixed in flexion. Roentgenography showed markedly narrow interphalangeal spaces of the proximal interphalangeal joints of the second to fourth fingers, bony fusion of the proximal interphalangeal joints of the fifth fingers. Abnormalities noted in the feet included brachymesophalangy, narrow joint gaps of the distal interphalangeal joints of the third toes, and ossiferous adhesion of the distal interphalangeal joints of the fourth and fifth toes (Fig. 1). The frontal skull base was flat, and the end plates of the lower thoracic and lumbar vertebrae were irregular. Joint arthroplasty was performed of the distal interphalangeal joints of the right second and third fingers.

At age 19 years, he measured 187 cm (+3.0 SD). He had a round and flat face, short palpebral fissures, arched eyebrows, hypertelorism, narrow forehead, low nasal bridge and abnormal ears. Anosmia was not noted. His pubic hair was rudimentary and his testes and penis were at Tanner Stage 2. His voice was high pitched. He had moderate mental retardation. He was able to add and subtract single-digit numbers. He attended primary school, and then a special class for handicapped children. He works at a confectionery factory and enjoys interaction with coworkers.

Radiography showed delayed closure of epiphyseal lines of the distal radii, carpal bones and phalanges. Hormonal studies showed low testosterone secretion associated with low gonadotropins, findings compatible with hypogonadotropic hypogonadism. Plasma levels of the following hormones were all reduced: testosterone 18.1 ng/dl (normal range: 270–1,070 ng/dl), luteinizing hormone 0.2 mIU/ml (1.8–5.2 mIU/ml), follicle-stimulating hormone 1.2 mIU/ml (2.9–8.2 mIU/ml), 17-ketosteroids 0.44 mg/dl (4.6–18.0 mg/dl), and 17-OH-corticosteroids 0.4 mg/dl (3.4–12.0 mg/dl). His response to androgen treatment was poor.

Cytogenetic and Molecular Cytogenetic Analysis

G-banded lymphocyte chromosomes of the boy showed an apparently balanced translocation 46,XY,t(10;17)(p15.3;q22) (Fig. 2). His mother had a normal karyotype, but his father refused to cooperate. FISH analysis of the translocation breakpoints was carried out using metaphase chromosomes from EB virus-transformed lymphoblastoid cells. Five bacterial artificial chromosome (BAC) clones mapped to 10p15.3 and another 10 clones at 17q22 were used in the analysis (Map viewer database, http://genome.ucsc.edu/). RP11-91E2

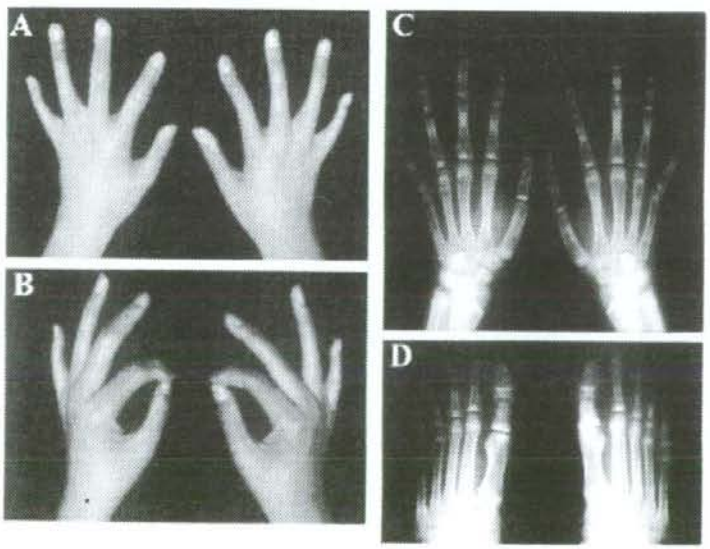

FIG. 1. Patient's hands and feet at age 13 years. **A**: Absence of creases on dorsal surface of proximal interphalangeal joints. **B**: Limited flexion of proximal interphalangeal joints. **C,D**: Radiographs showing narrowing and ossiferous adhesion of interphalangeal joints.

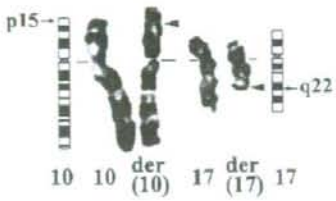

FIG. 2. G-banded partial karyotype of the patient with an apparently balanced translocation t(10;17)(p15;q22). Arrows indicate translocation points.

(10q26.3) and RP11-102N8 (17p13.3) served as controls. Clones 367C1, 9G4, 649B10 (containing the *NOG* gene), and 826B22 at 17q22 were deleted, with an estimated deletion segment at 2.8–3.7 Mb (Figs. 3 and 4). None of the 10p15 clones analyzed was deleted, with clone 15D19 spanning the 10p15 translocation breakpoint.

DISCUSSION

We report on a 19-year-old male with an apparently balanced translocation t(10;17)(p15.3;q22) and multiple synostosis syndrome 1, mild facial dysmorphism and moderate mental retardation. Chromosomal FISH analysis demonstrated a cryptic, 2.2–3.9 Mb deletion at 17q22 encompassing *NOG*, a gene responsible for multiple synostosis syndrome 1. It was therefore assumed that deletion of *NOG* in the patient was responsible for the syndrome. It is noteworthy that symphalangism has been described in six of six patients in the literature with deletions involving 17q22 or its vicinity [Park et al., 1992; Dallapiccola et al., 1993; Khalifa et al., 1993; Levin et al., 1995; Thomas et al., 1996; Mickelson et al., 1997; Marsh et al., 2000].

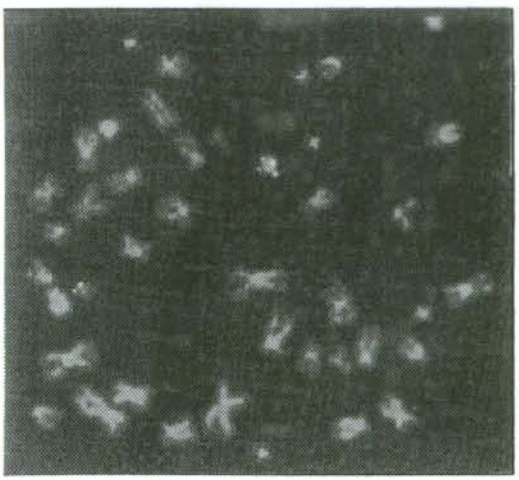

FIG. 3. FISH analysis using BAC clone 649B10 (17q22; red signal) which contains the *NOG* gene, and a chromosome 17 marker (RP11-102N8 at 17p13.3; green signal). Only one red signal is seen.

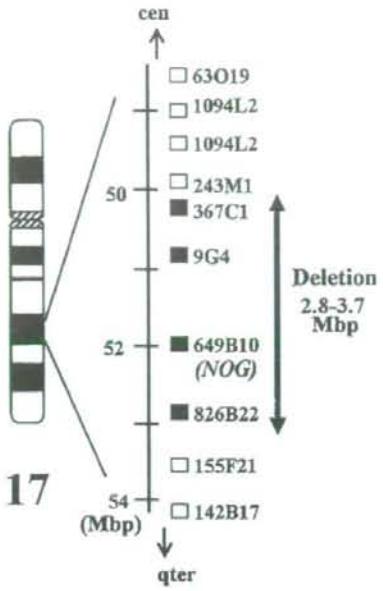

FIG. 4. Schematic representation of the deleted region around the 17q22 breakpoint along with physical map for BAC clones used for FISH. Open boxes (□) indicate non-deleted clones while closed boxes and (■) indicate deleted clones.

The boy developed hypogonadotropic hypogonadism, as evidenced by delayed puberty, tall stature, and decreased gonadotropic hormones. As mentioned earlier, at least four genes for hypogonadotropic hypogonadism have been described at 4q21, 8p11, 9q34, and 19p. It is likely that in the patient another gene for pituitary secretion of gonadotropic hormones was deleted in the 2.2–3.9 Mb interval at 17q22, although the possibility of its deletion at an additional cryptic rearrangement distant from the translocation breakpoints cannot be excluded [De Gregori et al., 2007].

ACKNOWLEDGMENTS

The authors wish to thank Dr. Gen Nishimura for valuable comments. This research was supported by Grants on Children and Families (H18-005) from the Ministry of Health, Labour and Welfare of Japan; and the Kawano Masanori Memorial Foundation for Promotion of Pediatrics, Japan.

REFERENCES

Bugge M, Bruun-Petersen G, Brondum-Nielsen K, Friedrich U, Hansen J, Jensen G, Jensen PK, Kristoffersson U, Lundsteen C, Niebuhr E, Rasmussen KR, Rasmussen K, Tommerup N. 2000. Disease associated balanced chromosome rearrangements: A resource for large scale genotype-phenotype delineation in man. J Med Genet 37:858–865.

Dallapiccola B, Mingarelli R, Digilio C, Obregon MG, Giannotti A. 1993. Interstitial deletion del(17) (q21.3q23 or 24.2) syndrome. Clin Genet 43:54–55.

De Gregori M, Ciccone R, Magini P, Pramparo T, Gimelli S, Messa J, Novara F, Vetro A, Rossi E, Maraschio P, Bonaglia MC, Anichini C, Ferrero GB, Silengo M, Fazzi E, Zatterale A, Fischetto R, Previderé C, Belli S, Turci A, Calabrese G, Bernardi F, Meneghelli E, Riegel M, Rocchi M, Guerneri S, Lalatta F, Zelante L, Romano C, Fichera M, Mattina T, Arrigo G, Zollino M, Giglio S, Lonardo F, Bonfante A, Ferlini A, Cifuentes F, Van Esch H, Backx L, Schinzel A, Vermeesch JR, Zuffardi O. 2007. Cryptic deletions are a common finding in "balanced" reciprocal and complex chromosome rearrangements: A study of 59 patients. J Med Genet 44: 750–762.

de Roux N, Young J, Misrahi M, Genet R, Chanson P, Schaison G, Milgrom E. 1997. A family with hypogonadotropic hypogonadism and mutations in the gonadotropin-releasing hormone receptor. N Engl J Med 337:1597–1602.

Gribble SM, Prigmore E, Burford DC, Porter KM, Ng BL, Douglas EJ, Fiegler H, Carr P, Kalaitzopoulos D, Clegg S, Sandstrom R, Temple IK, Youings SA, Thomas NS, Dennis NR, Jacobs PA, Crolla JA, Carter NP. 2005. The complex nature of constitutional de novo apparently balanced translocations in patients presenting with abnormal phenotypes. J Med Genet 42:8–16.

Khalifa MM, MacLeod PM, Duncan AM. 1993. Additional case of de novo interstitial deletion del(17)(q21.3q23) and expansion of the phenotype. Clin Genet 44:258–261.

Levin ML, Shaffer LG, Lewis R, Gresik MV, Lupski JR. 1995. Unique de novo interstitial deletion of chromosome 17, del(17) (q23.2q24.3) in a female newborn with multiple congenital anomalies. Am J Med Genet 55:30–32.

Marsh AJ, Wellesley D, Burge D, Ashton M, Browne C, Dennis NR, Temple K. 2000. Interstitial deletion of chromosome 17 (del(17)(q22q23.3)) confirms a link with oesophageal atresia. J Med Genet 37:701–704.

Mickelson EC, Robinson WP, Hrynchak MA, Lewis ME. 1997. Novel case of del(17)(q23.1q23.3) further highlights a recognizable phenotype involving deletions of chromosome (17)(q21q24). Am J Med Genet 71:275–279.

Miura K, Acierno JS Jr, Seminara SB. 2004. Characterization of the human nasal embryonic LHRH factor gene, NELF, and a mutation screening among 65 patients with idiopathic hypogonadotropic hypogonadism (IHH). J Hum Genet 49: 265–268.

Park JP, Moeschler JB, Berg SZ, Bauer RM, Wurster-Hill DH. 1992. A unique de novo interstitial deletion del(17)(q21.3q23) in a phenotypically abnormal infant. Clin Genet 41:54–56.

Pitteloud N, Acierno JS Jr, Meysing A, Eliseenkova AV, Ma J, Ibrahimi OA, Metzger DL, Hayes FJ, Dwyer AA, Hughes VA, Yialamas M, Hall JE, Grant E, Mohammadi M, Crowley WF Jr. 2006. Mutations in fibroblast growth factor receptor 1 cause both Kallmann syndrome and normosmic idiopathic hypogonadotropic hypogonadism. Proc Natl Acad Sci USA 103: 6281–6286.

Seminara SB, Messager S, Chatzidaki EE, Thresher RR, Acierno JS Jr, Shagoury JK, Bo-Abbas Y, Kuohung W, Schwinof KM, Hendrick AG, Zahn D, Dixon J, Kaiser UB, Slaugenhaupt SA, Gusella JF, O'Rahilly S, Carlton MB, Crowley WF Jr, Aparicio SA, Colledge WH. 2003. The GPR54 gene as a regulator of puberty. N Engl J Med 349:1614–1627.

Thomas JA, Manchester DK, Prescott KE, Milner R, McGavran L, Cohen MM Jr. 1996. Hunter-McAlpine craniosynostosis phenotype associated with skeletal anomalies and interstitial deletion of chromosome 17q. Am J Med Genet 62:372–375.

RESEARCH ARTICLE

AMERICAN JOURNAL OF
medical genetics

A Patient With Early Onset Huntington Disease and Severe Cerebellar Atrophy

Satoru Sakazume,[1,2]* Satoshi Yoshinari,[3] Eiji Oguma,[4] Emi Utsuno,[5] Takuma Ishii,[5] Yoko Narumi,[2] Takashi Shiihara,[2] and Hirofumi Ohashi[6]

[1]Division of Medical Genetics, Gunma Children's Medical Center, Gunma, Japan

[2]Division of Neurology, Gunma Children's Medical Center, Gunma, Japan

[3]Division of Neurology, Saitama Children's Medical Center, Saitama, Japan

[4]Division of Radiology, Saitama Children's Medical Center, Saitama, Japan

[5]Division of Genetic Counseling, Chiba University Hospital, Chiba, Japan

[6]Division of Medical Genetics, Saitama Children's Medical Center, Saitama, Japan

Received 6 June 2008; Accepted 11 December 2008

We report on a girl with early onset Huntington disease (HD). Her initial symptoms at 2 years of age included oral motor dysfunction and gait disturbance. Magnetic resonance imaging of the head revealed severe atrophy of both the vermis and the cerebellar cortex in addition to the common findings of basal ganglia including the caudate nuclei, putamen, and globus pallidus. Molecular analysis showed 160 CAG repeats in the *HD* gene. This mutation was inherited from her mother who was also affected, with a *HD* CAG expansion of 60 repeats. Cerebellar symptoms should be considered as a manifestation of early onset HD.

Key words: juvenile Huntington disease; CAG repeat; maternal expansion; cerebellar atrophy

How to Cite this Article:
Sakazume S, Yoshinari S, Oguma E, Utsuno E, Ishii T, Narumi Y, Shiihara T, Ohashi H. 2009. A patient with early onset Huntington disease and severe cerebellar atrophy.
Am J Med Genet Part A 9999:1–4.

INTRODUCTION

Huntington disease (HD) is a neurodegenerative disorder usually diagnosed in adulthood on the basis of symptoms of involuntary movement and a change in character. The disorder is caused by the expansion of the 5′ CAG repeat of the *HD* gene, and paternal anticipation is common. Early onset Huntington disease (EOHD), with an onset before 20 years of age, is estimated to account for only approximately 7% of all patients with HD, and patients for whom the age of onset is before 10 years constitute less than 1% of all patients with HD [Nance and Myers, 2001]. The clinical features of EOHD remarkably differ from those of adult-onset HD and are characterized by rigidity, oral motor dysfunction, ataxic gait, behavioral disturbance, and seizures [Rasmussen et al., 2000; Gonzalez-Alegre and Afifi, 2006; Yoon et al., 2006]. The CAG expansion in EOHD is greater than that in adult HD, and the prognosis of EOHD is generally unfavorable. Here, we describe a patient with EOHD and severe cerebellar cortical atrophy.

CLINICAL REPORT

The patient (female) was born at term following an uneventful pregnancy. Her birth weight was 2,690 g (−0.8 SD) and length was 46 cm (−1 SD). During the first year of life, her growth and development was normal. She lifted her head and chest by herself at 3 months of age; walked with hands held and stood up independently at 12 months; and ran well, walked up and down, jumped independently, and put three words together at 2 years. Since then she has been gradually exhibiting symptoms of motor regression, difficulty in speech, and frequent temper tantrums. When we examined her at the age of 3 years and 8 months, she spoke only

Additional Supporting Information may be found in the online version of this article.

Grant sponsor: Ministry of Health, Labor and Welfare of Japan; Grant sponsor: Kawano Masanori Memorial Foundation for Promotion of Pediatrics.

*Correspondence to:
Satoru Sakazume, Division of Medical Genetics, Gunma Children's Medical Center, Shimohakoda 779, Hokkitu, Shibukawa, Gunma 377-8577, Japan. E-mail: saka377@gcmc.pref.gunma.jp

Published online 00 month 2009 in Wiley InterScience (www.interscience.wiley.com)
DOI 10.1002/ajmg.a.32707

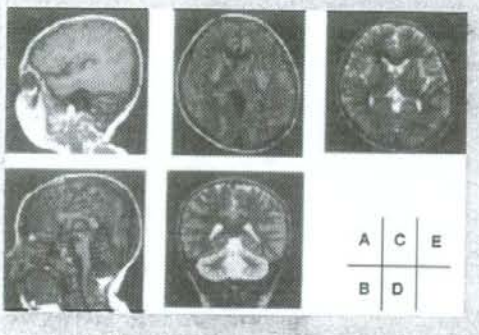

FIG. 1. A magnetic resonance image of the patient's brain at the age of 4 years. The sagittal (B) and the coronal (D) sections reveal cerebellar atrophy. E: The transverse section of a T2-weighted image shows atrophy of the globus pallidus. A,C: No significant cortical change was noted in cerebral gray or white matter.

single words and walked unstably with a wide gait. Three months later, she started having repeated and prolonged generalized tonic seizures and frequent falls. An electroencephalogram revealed bilateral sporadic spikes in the occipital areas. Magnetic resonance imaging (MRI) of the head revealed severe cerebellar atrophy in the vermis and cortex in addition to atrophy in the nuclei caudati, putamen, and globus pallidus (Fig. 1). Family history revealed that her mother, grandparent, and great grandparent were affected with HD.

MOLECULAR GENETIC ANALYSIS

In brief, genomic DNA was extracted from peripheral blood samples that were collected from the patient and her mother by using standard methods. Polymerase chain reaction (PCR) was performed according to a protocol described elsewhere by using the FAM-labeled forward primer ATG AAG GCC TTC GAG TCC CTC AAG TCC TTC and non-labeled reverse primer AAA CTC ACG GTC GGT GCA GCG GCT CCT CAG to span both ends of the repeat in the *HD* gene [Huntington's Disease Collaborative Research Group, 1993]. The PCR reaction of 25 μl consists of forward and reverse primers (1.0 pmol each), 0.4 mM dNTPs, 1xCG buffer (TaKaRa[Q1]), TaKaRa LA *Taq* polymerase (1.0 U) (TaKaRa), 200 ng of genomic DNA. Reactions were performed in ABI9700 thermal cycler for 1 cycle at 95°C for 5 minutes, 35 cycle at 95°C for 1 min, 60°C for 2 min, 68°C for 1.5 min. One microliter of a 1:5 dilution of reaction products was added to 12 μl of formamide (Hi-Di formamide, Applied Biosystems, Inc.[Q2]) and 0.5 μl of GS1000-ROX internal molecular weight standard (Applied Biosystems, Inc.), denatured at 95°C for 2 min, and immediately placed on ice for a minimum of 3 min. Amplicon length was analyzed by ABI PRISM 310 Genetic analyzer and Genescan software (Applied Biosystems, Inc.). The CAG expansion of the patient and her mother were confirmed to be 160 and 60 repeats respectively.

DISCUSSION

To our knowledge, the girl described here is one of the youngest patients with EOHD. We wish to emphasize the following two issues: maternal transmission of the mutant allele and cerebellar pathology. HD is inherited in an autosomal dominant pattern; both paternal and maternal transmission is possible. Paternal anticipation is the rule in HD [Ranen et al., 1995]. We reviewed seven reports of EOHD patients with over 100 repeats in the *HD* gene (Table I) [Nance et al., 1999; Gambardella et al., 2001; Milunsky et al., 2003; Seneca et al., 2004; Nahhas et al., 2005; Papapetropoulos et al., 2005]. In four patients, the mother transmitted the expanded allele and the maternal ages at the time of pregnancy were relatively young, ranging from 20 to 27 years [Nance et al., 1999; Nahhas et al., 2005; Papapetropoulos et al., 2005]. The age of the mothers when they had first experienced an HD symptom ranged from 16 to the early 20s. The incidence of maternal transmission in EOHD seems to be higher than that in the case of adult onset HD. Moreover, anticipation in maternal transmissions is seen in almost half of patients with EOHD having over 100 CAG repeats.

In two studies on adult onset HD, over 80 patients were screened for brain atrophy, and no significant cerebellar changes were detected [Jech et al., 2007; Ruocco et al., 2008]. However, among the seven reports of EOHD, cerebellar atrophy was confirmed in three patients (Table I) [Milunsky et al., 2003; Seneca et al., 2004]. In particular, progressive cerebellar atrophy was demonstrated by serial MRI in Patient 4, at the age of 2 years, periventricular leukomalacia was noted on brain MRI; and at 6 years, severe cortical atrophy with dilated ventricle and cerebellar atrophy were confirmed [Seneca et al., 2004]. We assume that the cerebellar change of the present patient is atrophy rather than hypoplasia.

Furthermore, Ribai et al. [2007] summarized the cases of 29 patients with HD. The incidence of maternal transmission was 25%, and cerebellar atrophy was identified in one patient. We observed that the incidences of maternal transmission and those of cerebellar atrophy are different between Ribai's report and our accumulated data (Table I).

In conclusion, anticipation in maternal transmissions is seen in half of very young onset cases with repeat number over 100. But it is important to note that this high maternal transmission rate might be overestimated because the patients with maternal transmission are more likely to be reportable. In addition, cerebellar atrophy is not a common, but a notable finding in EOHD, which might be progressive in some patients.

ACKNOWLEDGMENTS

We are grateful for the cooperation of the patients and their families in the present study. This work was supported in part by a grant for Research on Children and Families from the Ministry of Health, Labor and Welfare of Japan, and from Kawano Masanori Memorial Foundation for Promotion of Pediatrics.

TABLE I. Clinical Presentation of JHD With Family History

Refs.	Gender	Age at onset (years)	CAG repeat of the patient	Symptoms of the patient	Involvement of the brain	Transmission	Mutation of parent	Symptoms of parent	Maternal age at pregnancy (years)
Nance et al. [1999]	Male	2	250	Rigidity, seizure, drooling	Autopsy examination at 16 years revealed global cerebral atrophy. The cerebellum, midbrain, and brainstem changes were unremarkable histologically	Maternal	Mother; not tested	Mother developed depression and attempted suicide at age 16 years.	23
Gambardella et al. [2001]	Female	6	115	Seizure, cognitive failure, ataxia	Not described	Paternal	Father; not tested	Not described	—
Milunsky et al. [2003]	Female	1.5	256	Dystonia, speech impairment	At 3.5 years, cerebellar atrophy of the vermis, hemisphere, and peduncle	Paternal	Adopted when a neonate, not described by genetic test	Not described	—
Seneca et al. [2004]	Female	3	214	Seizure, psychomotor regression, diplegia	At 6 years, progressive cerebellar atrophy was confirmed	Paternal	CAG repeat of father: 54	Typical adult HD phenotype	—
Papapetropoulos et al. [2005]	Male	3.5	108	Cognitive failure, speech impairment, dystonia, ataxia,	Not described	Maternal	Not described	Patient's mother was first affected with HD at 23 years.	21
Nahhas et al. [2005]	Female	3.5	130–150	Speech impairment, ataxia,	At postmortem examination, mild cortical atrophy and moderately severe atrophy of the caudate and putamen were noted	Maternal	CAG repeat of mother: 70–90	Mother had symptoms of HD at 18 years	20
Present patient	Female	3	160	Rigidity, ataxia, cognitive failure, seizure, speech impairment	Severe cerebellar atrophy in the vermis and cortex as well as atrophy in the nuclei caudati, putamen, and globus pallidus	Maternal	CAG repeat of mother: 60	Mother was first affected with HD in her late 20s after delivery of the patient	27

REFERENCES

Gambardella A, Muglia M, Labate A, Magariello A, Gabriele AL, Mazzei R, Pirritano D, Conforti FL, Patitucci A, Valentino P, Zappia M, Quattrone A. 2001. Juvenile Huntington's disease presenting as progressive myoclonic epilepsy. Neurology 57:708–711.

Gonzalez-Alegre P, Afifi AK. 2006. Clinical characteristics of childhood-onset (juvenile) Huntington disease: Report of 12 patients and review of the literature. J Child Neurol 21:223–229.

Huntington's Disease Collaborative Research Group. 1993. A novel gene containing a trinucleotide repeat that is expanded and unstable on Huntington's disease chromosomes. The Huntington's Disease Collaborative Research Group. Cell 72:971–983.

Jech R, Klempir J, Vymazal J, Zidovska J, Klempirova O, Ruzicka E, Roth J. 2007. Variation of selective gray and white matter atrophy in Huntington's disease. Mov Disord 22:1783–1789.

Milunsky JM, Maher TA, Loose BA, Darras BT, Ito M. 2003. XL PCR for the detection of large trinucleotide expansions in juvenile Huntington's disease. Clin Genet 64:70–73.

Nahhas FA, Garbern J, Krajewski KM, Roa BB, Feldman GL. 2005. Juvenile onset Huntington disease resulting from a very large maternal expansion. Am J Med Genet Part A 137A:328–331.

Nance MA, Myers RH. 2001. Juvenile onset Huntington's disease—Clinical and research perspectives. Ment Retard Dev Disabil Res Rev 7:153–157.

Nance MA, Mathias-Hagen V, Breningstall G, Wick MJ, McGlennen RC. 1999. Analysis of a very large trinucleotide repeat in a patient with juvenile Huntington's disease. Neurology 52:392–394.

Papapetropoulos S, Lopez-Alberola R, Baumbach L, Russell A, Gonzalez MA, Bowen BC, Singer C. 2005. Case of maternally transmitted juvenile Huntington's disease with a very large trinucleotide repeat. Mov Disord 20:1380–1383.

Ranen NG, Stine OC, Abbott MH, Sherr M, Codori AM, Franz ML, Chao NI, Chung AS, Pleasant N, Callahan C, et al. 1995. Anticipation and instability of IT-15 (CAG)n repeats in parent-offspring pairs with Huntington disease. Am J Hum Genet 57:593–602.

Rasmussen A, Macias R, Yescas P, Ochoa A, Davila G, Alonso E. 2000. Huntington disease in children: Genotype-phenotype correlation. Neuropediatrics 31:190–194.

Ribai P, Nguyen K, Hahn-Barma V, Gourfinkel-An I, Vidailhet M, Legout A, Dode C, Brice A, Durr A. 2007. Psychiatric and cognitive difficulties as indicators of juvenile Huntington disease onset in 29 patients. Arch Neurol 64:813–819.

Ruocco HH, Bonilha L, Li LM, Lopes-Cendes I, Cendes F. 2008. Longitudinal analysis of regional grey matter loss in Huntington disease: Effects of the length of the expanded CAG repeat. J Neurol Neurosurg Psychiatry 79:130–135.

Seneca S, Fagnart D, Keymolen K, Lissens W, Hasaerts D, Debulpaep S, Desprechins B, Liebaers I, De Meirleir L. 2004. Early onset Huntington disease: A neuronal degeneration syndrome. Eur J Pediatr 163:717–721.

Yoon G, Kramer J, Zanko A, Guzijan M, Lin S, Foster-Barber A, Boxer AL. 2006. Speech and language delay are early manifestations of juvenile-onset Huntington disease. Neurology 67:1265–1267.

Q1: Please provide the manufacturers complete location.
Q2: Please provide the manufacturers complete location.

MOLECULAR AND CELLULAR BIOLOGY, Apr. 2008, p. 2125–2137 Vol. 28, No. 7
0270-7306/08/$08.00+0 doi:10.1128/MCB.00740-07

Inducible Expression of Chimeric EWS/ETS Proteins Confers Ewing's Family Tumor-Like Phenotypes to Human Mesenchymal Progenitor Cells▽†

Yoshitaka Miyagawa,[1] Hajime Okita,[1]* Hideki Nakaijima,[1] Yasuomi Horiuchi,[1] Ban Sato,[1] Tomoko Taguchi,[1] Masashi Toyoda,[3] Yohko U. Katagiri,[1] Junichiro Fujimoto,[2] Jun-ichi Hata,[1] Akihiro Umezawa,[3] and Nobutaka Kiyokawa[1]

Department of Developmental Biology, National Research Institute for Child Health and Development, 2-10-1, Okura, Setagaya-ku, Tokyo 157-8535, Japan[1]; National Research Institute for Child Health and Development, 2-10-1, Okura, Setagaya-ku, Tokyo 157-8535, Japan[2]; and Department of Reproductive Biology, National Research Institute for Child Health and Development, 2-10-1, Okura, Setagaya-ku, Tokyo 157-8535, Japan[3]

Received 27 April 2007/Returned for modification 13 July 2007/Accepted 7 January 2008

Ewing's family tumor (EFT) is a rare pediatric tumor of unclear origin that occurs in bone and soft tissue. Specific chromosomal translocations found in EFT cause EWS to fuse to a subset of ets transcription factor genes (ETS), generating chimeric EWS/ETS proteins. These proteins are believed to play a crucial role in the onset and progression of EFT. However, the mechanisms responsible for the EWS/ETS-mediated onset remain unclear. Here we report the establishment of a tetracycline-controlled EWS/ETS-inducible system in human bone marrow-derived mesenchymal progenitor cells (MPCs). Ectopic expression of both EWS/FLI1 and EWS/ERG proteins resulted in a dramatic change of morphology, i.e., from a mesenchymal spindle shape to a small round-to-polygonal cell, one of the characteristics of EFT. EWS/ETS also induced immunophenotypic changes in MPCs, including the disappearance of the mesenchyme-positive markers CD10 and CD13 and the up-regulation of the EFT-positive markers CD54, CD99, CD117, and CD271. Furthermore, a prominent shift from the gene expression profile of MPCs to that of EFT was observed in the presence of EWS/ETS. Together with the observation that EWS/ETS enhances the ability of cells to invade Matrigel, these results suggest that EWS/ETS proteins contribute to alterations of cellular features and confer an EFT-like phenotype to human MPCs.

Ewing's family tumor (EFT) is a rare childhood cancer arising mainly in bone and soft tissue. Since EFT has a poor prognosis, it is important to elucidate the underlying pathogenic mechanisms for establishing a more effective therapeutic strategy. EFT is characterized by the presence of chimeric genes composed of EWS and ets transcription factor genes (ETS) formed by specific chromosomal translocations, i.e., EWS/FLI1, t(11;22)(q24;q12); EWS/ERG, t(21;22)(q12;q12); EWS/ETV1, t(7;22)(p22;q12); EWS/E1AF, t(17;22)(q12;q12); and EWS/FEV, t(2;22)(q33;q12) (26). The products of these chimeric genes behave as aberrant transcriptional regulators and are believed to play a crucial role in the onset and progression of EFT (3, 36). Indeed, recent studies have revealed that the induction of EWS/FLI1 proteins can trigger transformation in certain cell types, including NIH 3T3 cells (36), C2C12 myoblasts (12), and murine primary bone marrow-derived mesenchymal progenitor cells (MPCs) (6, 45, 52). However, studies have also indicated that overexpression of EWS/FLI1 provokes apoptosis and growth arrest in mouse normal embryonic fibroblasts and primary human fibroblasts (10, 31), hence hampering understanding of the precise role of EWS/ETS proteins in the development of EFT. The function of EWS/ETS proteins would be greatly influenced by cell type, and thus the cells that can originate EFTs might be more susceptible to the tumorigenic effects of EWS/ETS.

Although the cell origin of EFT is still unknown, the expression of neuronal markers in spite of the occurrence in bone and soft tissues has kept open the debate as to a potential mesenchymal or neuroectodermal origin. As described above, ectopic expression of EWS/FLI1 results in dramatic changes in morphology and the formation of EFT-like tumors in murine primary bone marrow-derived MPCs but not in murine embryonic stem cells (6, 45, 52), supporting the notion that MPCs are a plausible cell origin of EFT (45). However, others argue that MPCs cannot be considered progenitors of EFT without further evidence of similarity between human EFT and MPC-EWS/FLI1-induced tumors in mice (29, 46).

The development of experimental systems using murine species is useful for elucidating the mechanisms behind the pathogenesis of EFT. However, several differences between human and murine systems cannot be ignored; these differences include the expression patterns of surface antigens in MPCs, for instance (7, 44, 51, 53). Moreover, human cells are difficult to transform in vitro, and the transformed cells of mice seem to produce a more aggressive tumor than those of hu-

* Corresponding author. Mailing address: Department of Developmental Biology, National Research Institute for Child Health and Development, 2-10-1, Okura, Setagaya-ku, Tokyo 157-8535, Japan. Phone: 81-3-3416-0181. Fax: 81-3-3417-2496. E-mail: okita@nch.go.jp.

† Supplemental material for this article may be found at http://mcb.asm.org/.

▽ Published ahead of print on 22 January 2008.

TABLE 1. Cell lines used in this study and fusion transcript types

Cell line	Diagnosis	Fusion transcript type	Reference
EES-1	EFT	EWS/FLI1 type I	20
SCCH196	EFT	EWS/FLI1 type I	21
RD-ES	EFT	EWS/FLI1 type II	5
SK-ES1	EFT	EWS/FLI1 type II	5
NCR-EW2	EFT	EWS/FLI1 type II	19
NCR-EW3	EFT	EWS/E1AF	19
W-ES	EFT	EWS/ERG	13
NB69	NB		15
NB9	NB		15
GOTO	NB		47
NRS-1	RMS	PAX3/FKHR	40

mans (1). The findings suggest the existence of undefined cell-autonomous mechanisms that render human cells resistant to malignant transformation. Therefore, the use of human cell models is ideal for clarifying how EFT develops. Models of the onset of EFT have been generated using primary fibroblasts (31) and rhabdomyosarcoma cells (23). However, these cell types are not appropriate for studying the origins of EFT, and a model that precisely recapitulates EWS/ETS-mediated EFT formation is required.

UET-13 cells are obtained by prolonging the life span of human bone marrow stromal cells by use of the retroviral transgenes hTERT and E7 (38, 50), retain the ability to differentiate into not only mesodermal derivatives but also neuronal progenitor-like cells, and are considered a good model for studying the cellular events in human MPCs. Therefore, we have examined the biological effect of EWS/ETS in human MPCs by use of UET-13 cells by exploiting tetracycline-inducible systems for expressing EWS/ETS (EWS/FLI1 and EWS/ERG). Here we report that overexpression of EWS/ETS mediates an EFT-like phenotype, including morphology, immunophenotype, and gene expression profile, with enhancement of the Matrigel invasion ability of UET-13 cells.

MATERIALS AND METHODS

Cell cultures and establishment of UET-13TR-EWS/ETS cell lines. UET-13 cells were cultured in Dulbecco's modified Eagle's medium (DMEM) with 10% Tet system approved fetal bovine serum (T-FBS) (Takara) at 37°C under a humidified 5% CO_2 atmosphere. EFT cell lines (EES-1 [20], SCCH196 [21], RD-ES and SK-ES1 [5], NCR-EW2 and NCR-EW3 [19], and W-ES [13]) and neuroblastoma (NB) cell lines (NB69 and NB9 [15] and GOTO [47]) were cultured in RPMI 1640 with 10% FBS. A rhabdomyosarcoma cell line, NRS-1 (40), was cultured in Eagle's minimal essential medium with 10% FBS. The cell lines used in this study are listed in Table 1.

UET-13 cells were seeded at a density of 5×10^4 cells per well in 24-well tissue culture plates 1 day prior to transfection. For introducing the tetracycline-inducible system, UET-13 cells were transfected with pcDNA6-TR (Invitrogen) by use of Lipofectamine 2000 (Invitrogen). After 72 h, the medium was replaced with fresh medium containing 200 μg/ml of blasticidin S (Invitrogen). Individual resistant clones were selected for a month and designated UET-13TR cells. UET-13TR cells were further transfected with pcDNA4-EWS/ETSs constructed as described below, and individual resistant clones were selected in DMEM containing 10% T-FBS and 200 to 300 μg/ml of Zeocin (Invitrogen). The Zeocin-resistant clones were expanded and tested for the induction of EWS/ETS expression upon the addition of tetracycline by use of reverse transcription-PCR (RT-PCR) as described below.

Plasmid construction. A gateway cassette (bases 1 to 1705) was amplified from pBLOCK-iT3-DEST (Invitrogen) by PCR, and the PCR product was inserted into the EcoRV site of pcDNA4-TO (Invitrogen) (termed pcDNA4-DEST). Since the type II EWS/FLI1 is a stronger transactivator than the type I product (32), we used the type II variant in the present study. EWS/ERG was isolated from W-ES, an EFT cell line, joining EWS exon 7 and ERG exon 9. Full-length EWS/FLI1 type II and EWS/ERG cDNAs were amplified from cDNAs prepared from NCR-EW2 and W-ES cells, respectively, by PCR as described below and cloned into the XmnI-EcoRV sites of pENTR11 (Invitrogen). The resulting pENTR11-EWS/ETSs were recombined with pcDNA4-DEST by use of LR recombination reaction as instructed by the manufacturer (Invitrogen) to construct the tetracycline-inducible EWS/ETS expression vector pcDNA4-EWS/ETSs.

Western blot analysis. UET-13 transfectants were cultivated with or without 3 μg/ml of tetracycline for 72 h. Western blot analysis was performed as previously described (37). Briefly, the cell lysates were prepared and separated on a 10% sodium dodecyl sulfate-polyacrylamide gel electrophoresis gel and transferred onto a polyvinylidene difluoride membrane. The membranes were blocked with 5% skimmed milk in phosphate-buffered saline (PBS) containing 0.01% Tween 20 (Sigma) and incubated with primary antibodies. As the primary antibodies, anti-Fli-1, anti-Erg-1/2/3 (Santa Cruz Biotechnology), and anti-actin (Sigma) were used. Horseradish peroxidase-conjugated anti-rabbit or anti-mouse immunoglobulin G (IgG) antibodies (DakoCytomation) were used as secondary antibodies. Blots were detected by chemiluminescence using an ECL Plus Western blotting detection system (GE Healthcare Bio-Science Corp.) and exposed to X-ray film (Kodak) for 5 to 30 min.

MTT assay and detection of apoptosis. Growth curves of UET-13 transfectants were determined using the 3-(4,5-dimethylthiazol-2-yl)-2,5-diphenyltetrazolium bromide (MTT) assay as described previously (18). The apoptosis was detected using an annexin V-fluorescein isothiocyanate (FITC) apoptosis detection kit (Biovision) according to the manufacturer's instructions and analyzed by flow cytometry (Cytomics FC500; Beckman Coulter).

Immunofluorescence analysis. After 1 week of culture in the absence or presence of tetracycline, UET-13 cells and the transfectants were harvested with 0.25% trypsin plus EDTA (IBL). The cells (2×10^5) were incubated with mouse monoclonal antibodies for 20 min. In the case of fluorescence-labeled antibodies, the cells were washed with PBS and then analyzed. In the case of primary unconjugated mouse antibodies, the cells were washed and then incubated with FITC-conjugated goat anti-mouse IgG antibody (Jackson ImmunoResearch Laboratories) for 20 min. Cell fluorescence was detected using a Cytomics FC500 instrument as described previously (27).

Antibodies against the following human antigens were used: CD10, CD13, CD14, CD29, CD34, CD40, CD44, CD45, CD49e, CD54, CD56, CD61, CD90, CD105, CD117, and CD166 from Beckman Coulter; CD73 from BD Biosciences-Pharmingen; CD55 from Abcam; CD59 from Cedarlane Laboratories; and CD133 and CD271 from Miltenyi Biotec GmbH.

Immunocytochemistry. Cells were grown on collagen type I-coated cover glasses (Iwaki). After 72 h with or without tetracycline, cells were fixed for 30 min in 4% paraformaldehyde and permeabilized in PBS containing 0.2% Triton X-100 (Sigma) for 30 min. Subsequently, they were washed with PBS and blocked in PBS containing 0.1% Triton X-100 and 1% bovine serum albumin (Sigma) for 30 min before being incubated with a monoclonal anti-CD99 antibody, i.e., 12E7 (1:100) (DakoCytomation) or O13 (1:200) (Thermo), and polyclonal anti-Fli-1 antibody (1:100) (Santa Cruz) for 1 h. Bound antibodies were visualized with appropriate secondary antibodies, i.e., Alexa Fluor 488 goat anti-mouse IgG (heavy plus light chains) highly cross-adsorbed and Alexa Fluor 546 goat anti-rabbit IgG (heavy plus light chains) highly cross-adsorbed (Invitrogen) for 1 h at 1:300. Nuclei were counterstained with 4′,6′-diamidino-2-phenylindole (DAPI) or propidium iodide (PI) (Sigma). For the visualization of whole cells, cells were treated with Celltracker Blue (Invitrogen) for 30 min and then fixed. Fluorescence was observed and analyzed using a confocal laser scanning microscope and image software (either FV500 from Olympus or LSM510 from Carl Zeiss). Precise measurements of cell size, nuclear size, and the nucleus-to-cytoplasm (N/C) ratio were performed using Image J (16).

RT-PCR analysis. Total RNA was extracted from cells by use of an RNeasy kit (Qiagen) and reverse transcribed using a first-strand cDNA synthesis kit (GE Healthcare Bio-Science Corp). RT-PCR was performed with a HotstarTaq master mix kit (Qiagen). As an internal control, human GAPDH cDNA was also amplified. The sequences of gene-specific primers for RT-PCR were as follows: for EWS/FLI1 (forward), 5′-ATGGCGTCCACGGATTACAGTACCT-3′; for EWS/FLI1 (reverse), 5′-GGGTCTTCTTTGACACTCAATCG-3′; for EWS/ERG (forward), 5′-ATGGCGTCCACGGATTACAGTACCT-3′; for EWS/ERG (reverse), 5′-TTAGTAGTAAGTGCCCAGATGAGAA-3′; for GAPDH (forward), 5′-CCACCCATGGCAAATTCCATGGCA-3′; and for GAPDH (reverse), 5′-TCTAGACGGCAGGTCAGGT/CCACC-3′. PCR products were electrophoresed with a 1% agarose gel and stained with ethidium bromide.